EEL-1, a Hect E3 ubiquitin ligase, controls asymmetry and persistence of the SKN-1 transcription factor in the early *C. elegans* embryo

Barbara D. Page[1,2,3,*], Scott J. Diede[4], Jennifer R. Tenlen[1,5] and Edwin L. Ferguson[3,6]

During early divisions of the *C. elegans* embryo, many maternally supplied determinants accumulate asymmetrically, and this asymmetry is crucial for proper cell fate specification. SKN-1, a transcription factor whose message is maternally supplied to the embryo, specifies the mesendodermal cell fate. In the 2-cell embryo, SKN-1 is expressed at a higher level in the posterior cell. This asymmetry becomes more pronounced at the 4-cell stage, when SKN-1 is high in the posterior cell's daughters and low in the daughters of the anterior blastomere. To date, the direct mechanisms that control SKN-1 distribution remain unknown. In this report, we identify *eel-1*, which encodes a putative Hect E3 ubiquitin ligase that shares several domains of similarity to the mammalian E3 ligase Mule. EEL-1 binds SKN-1 and appears to target SKN-1 for degradation. EEL-1 has two functions in regulating SKN-1 during early embryogenesis. First, *eel-1* promotes the spatial asymmetry of SKN-1 accumulation at the 2- and 4-cell stages. Second, *eel-1* acts in all cells to downregulate SKN-1 from the 12- to the 28-cell stage. Although loss of *eel-1* alone causes a reduction in SKN-1 asymmetry at the 2-cell stage, the function of *eel-1* in both the spatial and temporal regulation of SKN-1 is redundant with the activities of other genes. These data strongly suggest that multiple, functionally redundant pathways cooperate to ensure precise control of SKN-1 asymmetry and persistence in the early embryo.

KEY WORDS: SKN-1, Hect ubiquitin ligase, Protein degradation, Cell fate specification, Asymmetric cell division

INTRODUCTION

The complexity of multicellular organisms arises, in part, from mechanisms that establish differences between sister cells. The early *C. elegans* embryo is an excellent system to study the molecular processes underlying asymmetric cell division. The single-celled *C. elegans* zygote divides to produce two blastomeres, each of which has a distinct developmental potential. The genetic analysis of this asymmetric division has provided fundamental insights into how polarity is established within a single cell and has led to the identification of several maternally supplied determinants that become asymmetrically expressed in descendant cells (Rose and Kemphues, 1998; Doe and Bowerman, 2001).

However, less is known about the specific mechanism(s) used to establish the asymmetry of these determinants. For those cases in which it has been investigated, a variety of processes, including translational regulation, protein stability and protein enrichment, have been shown to direct asymmetric protein accumulation (Rose and Kemphues, 1998; Bowerman, 2000; Doe and Bowerman, 2001). For example, at the 2-cell stage, GLP-1 protein is present only in the anterior cell owing to translational repression of *glp-1* mRNA in the posterior (Evans et al., 1994; Marin and Evans, 2003; Ogura et al., 2003). Conversely, PIE-1 protein becomes progressively more concentrated in the posterior of the embryo owing to a combination of protein elimination in the anterior and enrichment in the posterior (Reese et al., 2000; DeRenzo et al., 2003).

The SKN-1 protein was one of the first maternal determinants shown to be asymmetrically localized (Bowerman et al., 1993). *skn-1* encodes a transcription factor that is required for a subset of mesodermal cell types and is involved in the specification of endoderm (Bowerman et al., 1992). The *skn-1* message is transcribed in the maternal germline, but SKN-1 protein is not detected until after fertilization (Bowerman et al., 1993; Seydoux and Fire, 1994). At the 2-cell stage, *skn-1* mRNA appears to be evenly distributed between anterior and posterior cells (Seydoux and Fire, 1994); however, SKN-1 protein is more concentrated in the posterior cell than its anterior sister. At the 4-cell stage, SKN-1 asymmetry is even more pronounced; SKN-1 is low in daughters of the anterior blastomere and high in daughters of the posterior blastomere. After the 8-cell stage, SKN-1 protein is no longer detected in the early embryo (Bowerman et al., 1993). Misexpression of SKN-1 in the daughters of the anterior blastomere causes ectopic expression of certain mesoderm-determining genes, such as *med-1* (Maduro et al., 2001; Tenlen et al., 2006). The descendants of these anterior cells ultimately differentiate as pharyngeal tissue and body wall muscle instead of ectoderm (Mello et al., 1992; Schubert et al., 2000; Page et al., 2001). This phenotype is referred to as Mex (muscle excess).

Loss or reduction in function of any of four genes, *mex-1*, *mex-5*, *efl-1* or *dpl-1*, causes a mother to produce embryos with a Mex phenotype. These embryos have a disruption in the asymmetric pattern of SKN-1, such that SKN-1 is high in both the anterior and posterior blastomeres (Bowerman et al., 1993; Schubert et al., 2000; Page et al., 2001). However, the mechanisms by which these genes affect SKN-1 are not known. *mex-1* and *mex-5* encode proteins containing CCCH zinc-finger motifs (Guedes and Priess, 1997;

[1]Division of Basic Sciences, Fred Hutchinson Cancer Research Center and [2]Howard Hughes Medical Institute, Seattle, WA 98109, USA. [3]Department of Molecular Genetics and Cell Biology, University of Chicago, Chicago, IL 60637, USA. [4]Children's Hospital and Regional Medical Center, Department of Hematology and Oncology, Seattle, WA 98105, USA. [5]Molecular and Cellular Biology Program, University of Washington, Seattle, WA 98195, USA. [6]Committee on Developmental Biology, University of Chicago, Chicago, IL 60637, USA.

*Author for correspondence (e-mail: bdpage@gmail.com)

Schubert et al., 2000), and this class of proteins has been implicated in multiple aspects of mRNA regulation, including mRNA stability and translational repression (Lai et al., 1999; Ogura et al., 2003; Puig et al., 2005; Pagano et al., 2007). Thus, MEX-1 and MEX-5 could affect SKN-1 asymmetry at the level of translation or stability of the maternally supplied *skn-1* message.

efl-1 and *dpl-1* encode transcription factors analogous to mammalian E2F and its dimerization partner (DP), respectively (Page et al., 2001). Two lines of experiments indicate that the EFL-1–DPL-1 heterodimer has an indirect role in controlling SKN-1 accumulation in the embryo. First, temperature shift experiments and mosaic analysis indicate that EFL-1 functions in the transcriptionally active region of the maternal germline and not in the embryo itself (Page et al., 2001). Second, the EFL-1–DPL-1 heterodimer has been shown to upregulate transcription of several genes in the maternal germline, including *mex-1* and *mex-5* (Chi and Reinke, 2006). Most likely, it is reduced expression of these target genes that disrupts SKN-1 asymmetry in *efl-1* or *dpl-1* Mex mutants.

To identify additional genes responsible for the generation of SKN-1 asymmetry, we performed a traditional genetic modifier screen with the temperature-sensitive mutant *efl-1(se1)*. From this screen, we identified one Eel (enhancer of *efl-1*) mutation. *eel-1* encodes a protein predicted to be a Hect E3 ubiquitin ligase that contains multiple domains of similarity to the mammalian Mcl1 ubiquitin ligase Mule (also known as Huwe1) (Adhikary et al., 2005; Chen et al., 2005; Zhong et al., 2005). E3 ligases are the last enzymes in the ubiquitination cascade that targets proteins for degradation, and commonly confer substrate specificity to the ubiquitin pathway (Pickart, 2001; Kipreos, 2005). In a yeast two-hybrid assay, EEL-1 specifically interacts with the C-terminus of SKN-1, and this C-terminal domain can target GFP for EEL-1-dependent degradation in vivo at a stage similar to that when endogenous SKN-1 disappears from the early embryo. In *eel-1* single-mutant embryos, SKN-1 asymmetry is reduced at the 2-cell stage, but by the 4-cell stage these mutant embryos have a SKN-1 distribution similar to that of wild type. Thus, EEL-1 appears to directly target SKN-1 for degradation, and SKN-1 protein instability plays a role in generating its asymmetry. However, EEL-1 is not the only protein responsible for SKN-1 asymmetry, highlighting the necessity for functional redundancy in this crucial cellular process.

MATERIALS AND METHODS

Strains
The Bristol strain N2 was the wild-type strain. The following strains were used: mapping strains MT3751 and MT464; Hawaiian variant strain CB4856 for SNP mapping (Wicks et al., 2001); LG III, *unc-119(ed3)*; LG IV, *lin-1(e1275)*, *ric-8(md303)*, *eel-1(zu462)*, *unc-17(e113)*, *unc-33(e204)*, *dpy-13(e184)*; LG V, *efl-1(se1)*, *rol-4(sc8)* (also known as *sqt-3* – Wormbase); LG X, *lin-2(e1309)*, and a strain carrying the gene fusion *med-1::gfp* (Maduro et al., 2001). *C. elegans* culture, mutagenesis and genetics were performed as previously described (Brenner, 1974).

Screen for modifiers of *efl-1(se1)* and genetics of *eel-1(zu462)*
We screened for modifiers of *efl-1(se1)* (Tenlen et al., 2006). When outcrossing a strain containing a dominant suppressor, we recovered a recessive enhancer of *efl-1(se1)* present in the same strain. We mapped this enhancer to chromosome IV and named it *eel-1*.

The *eel-1(zu462)* allele acts as a maternal enhancer of *efl-1*. N2 males mated to *eel-1(zu462);efl-1(se1)* hermaphrodites produced in excess of 90% Mex progeny. Conversely, *eel-1(zu462)* males mated to *efl-1(se1)* hermaphrodites at 20°C produced in excess of 90% viable progeny. These genetic data indicated that *eel-1* is supplied maternally to the embryo.

Mapping and molecular characterization of *eel-1*
We mapped *eel-1* to chromosome IV between *ric-8* (–6.72) and *unc-33* (–3.55). Single nucleotide polymorphism (SNP) mapping placed *eel-1* in a 68,256 bp region between SNP Y54G2A 258506 and SNP Y67D8C 3076845 (Wicks et al., 2001). RNA interference (RNAi) against genes in this region was performed in an *efl-1(se1)* background. Only RNAi directed against the gene Y67D8C.5 gave a Mex phenotype.

To confirm that *eel-1* is the Y67D8C.5 gene, we sequenced this genomic region from our *zu462* mutant. Our sequence of wild-type *eel-1* was in agreement with the sequence of Y67D8C.5 (GenBank accession AC025724). In the *zu462* background, the Y67D8C.5 gene contained a complex disruption that included both a deletion and an inverted duplication of the sequence. The deletion would remove the coding region for amino acids 3103-3405. The inverted duplication was inserted at the codon for amino acid 3103 and would result in a predicted open reading frame for an additional 36 amino acids after amino acid 3102. The duplication was 5884 bp in length and corresponded to the region of Y67D8C.5 encoding amino acids 1427-3004.

RNA-mediated interference
For RNAi experiments, the following cDNAs were used: for *eel-1*, yk395b1, yk13c8 and yk1100d4; for Y54G2A.29, yk151d6 and yk828f6; for Y54G2A.3, yk717g5; for Y67D8C.3, yk248f4; for *smg-1*, yk1190g4; for *mex-1*, yk880f10; for *skn-1*, yk2d12. For *glp-1(RNAi)*, we used the *glp-1* plasmid designed for dsRNA feeding (Kamath and Ahringer, 2003). The inserts of the above plasmids were used as templates to generate dsRNA for each gene. For the genes Y67D8C.6 and Y67D8C.4, we used PCR to amplify a ~400 bp coding region from the genomic region of each and generated dsRNA against these products (sequence of the oligos available upon request). To specifically target *mex-5* or *mex-6* by RNAi, we generated dsRNA against the regions described by Schubert et al. (Schubert et al., 2000). We performed all RNAi experiments by soaking worms at the L4 stage in 3 μl of dsRNA for 16 hours. After soaking, worms were allowed to recover for 6 hours before progeny were analyzed.

Antibodies and immunofluorescence
Antibodies against the following proteins were used as previously described: SKN-1 (Bowerman et al., 1993), PGL-1 (Kawasaki et al., 1998), MEX-5 (Schubert et al., 2000) and PIE-1 (Tenenhaus et al., 1998). Pharyngeal muscle cells were recognized with antibody mAb3NB12 (Priess and Thomson, 1987) and expression of *med-1* was determined using a MED-1:GFP fusion (Maduro et al., 2001).

Quantitation of SKN-1 levels
To compare SKN-1 levels between different blastomeres of the same embryo and between equivalent blastomeres in embryos of different genotypes, we used a Zeiss Axioplan microscope equipped with a CCD camera (Photometrics CoolSnap, Roper Scientific) and CoolSnap software (v. 1.2.0, Roper Scientific). Nuclear SKN-1 staining was quantitated using ImageJ software (http://rsb.info.nih.gov/ij) and the integrated density of staining per unit area was determined. Statistical comparisons were calculated using a two-tailed two-sample *t*-test assuming unequal variances. To ensure accuracy of the direct comparison of SKN-1 levels in *eel-1(–)* blastomeres with the equivalent blastomeres in wild type, we compared embryos of both genotypes stained on the same slide. In this experiment, a GFP marker present in the otherwise wild-type strain allowed us to distinguish wild-type embryos from *eel-1(–)* embryos by co-staining for GFP. The presence of the GFP marker did not alter the level of SKN-1 staining.

Yeast two-hybrid assay
To test for interaction between EEL-1 and SKN-1, we generated multiple plasmids for the yeast two-hybrid assay. A longer *eel-1* cDNA was created by joining the cDNAs yk1100d4 and yk395b1. The region of *eel-1* encoding amino acids 975-2018 was fused to the gene encoding the GAL4 DNA-binding domain (pGBDU-C3). The region of *eel-1* encoding amino acids 3429-4177 was fused to the gene encoding the GAL4 DNA-binding domain (pGBDU-C1) using the *eel-1* cDNA yk1047c7. We fused the region of *skn-1* encoding amino acids 37-623 to the gene encoding the GAL4 activation domain (pGAD-C1) using the *skn-1* cDNA yk12d2. To narrow down regions

Table 1. *eel-1* enhancement of the *efl-1(se1)* phenotype

Maternal genotype	Mex (%)	Normal morphology (%)	Non-Mex D.E. (%)	*n*
Wild type (N2)	0	100	0	495
efl-1(se1)	0	96	4	339
eel-1(zu462)	0	88	12	262
eel-1(RNAi)	0	99	1	139
eel-1(zu462);efl-1(se1)	93	0	7	294
efl-1(se1);eel-1(RNAi)	85	5	10	255
eel-1(zu462)/+;efl-1(se1)	24	63	13	219
eel-1(zu462)/+;efl-1(se1);smg-1(RNAi)	90	7	3	835
efl-1(se1);smg-1(RNAi)	11	68	21	100
eel-1(zu462)/+;smg-1(RNAi)	0	100	0	50

D.E., dead embryo.
All hermaphrodites were incubated at 20°C. Normal morphology was assessed by the number of embryos that were pretzel-shaped (see Fig. 1).

of interaction between EEL-1 and SKN-1, we constructed four additional plasmids: EEL-1(975-1373 aa) and EEL-1(1307-2018 aa) in pGBDU-C1; SKN-1(37-244 aa) and SKN-1(298-623 aa) in pGAD-C1. These plasmids were transformed into yeast strain PJ69-4A in appropriate combinations. Interaction was tested by growth on synthetic complete plates lacking uracil, leucine and histidine and supplemented with 5 mM 3-amino-1,2,4-triazole (3-AT).

Construction and transformation of the GFP:SKN-1 fusion

We fused the coding region of *skn-1* from amino acids 298-623 in frame to the 3′ end of the *gfp* coding region in the plasmid pJT31. The pJT31 plasmid is a modification of a previously constructed plasmid (Strome et al., 2001). In this plasmid, the expression of GFP is under control of the *pie-1* promoter and *pie-1* 3′UTR, and the plasmid contains *unc-119(+)* allowing selection for *C. elegans* transformants (Maduro and Pilgrim, 1995). The GFP:SKN-1(298-623) construct was transformed into *unc-119(–)* worms using a microparticle bombardment apparatus with a HEPTA adapter (Praitis et al., 2001).
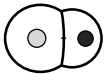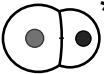
RESULTS

Loss-of-function of *eel-1* enhances *efl-1(se1)* to a Mex phenotype

To gain insight into how SKN-1 becomes asymmetric in the early embryo, we screened for modifiers of the temperature-sensitive mutant *efl-1(se1)*. At 20°C, *efl-1(se1)* mothers produce embryos with a wild-type SKN-1 expression pattern; the majority of these progeny are viable (Table 1 and Fig. 1). At 26°C, *efl-1(se1)* mothers produce embryos in which SKN-1 is abnormally high in the anterior blastomere and its daughters. As a consequence of SKN-1 misexpression, these embryos are inviable and have a terminal Mex phenotype (Page et al., 2001). From this modifier screen, we isolated an Eel (enhancer of *efl-1*) mutant (see Materials and methods). Whereas *eel-1(zu462)* single-mutant mothers produced non-Mex embryos that were viable at 20°C, a mother homozygous for both *eel-1(zu462)* and *efl-1(se1)* produced Mex
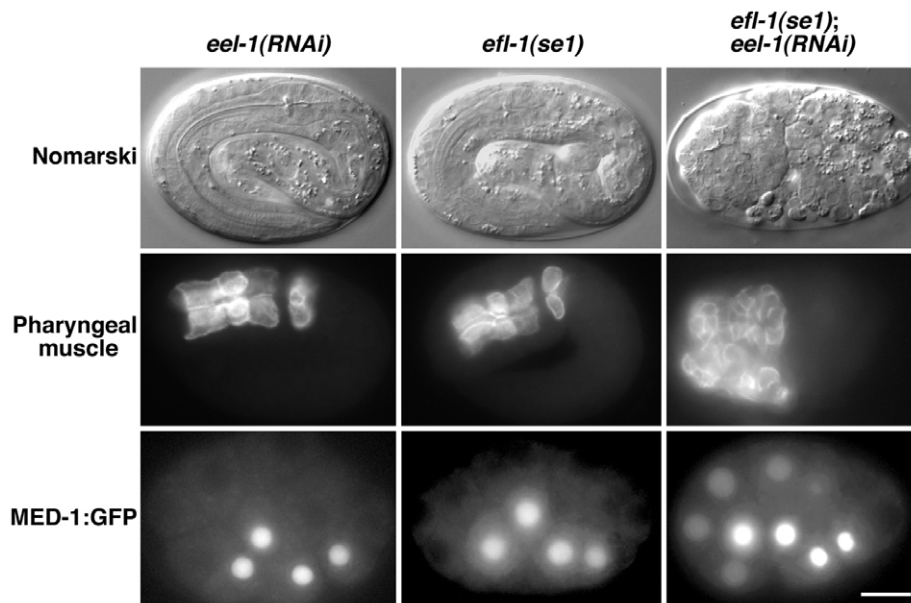
Fig. 1. Loss of *eel-1* enhances *efl-1(se1)* to a Mex phenotype. The top row contains Nomarski images of terminally developed *C. elegans* embryos from *eel-1(RNAi)*, *efl-1(se1)* and *efl-1(se1);eel-1(RNAi)* mothers incubated at 20°C. Note that *eel-1(RNAi)* and *efl-1(se1)* embryos form enclosed pretzel-shaped embryos and appear as wild type. By contrast, *efl-1(se1);eel-1(RNAi)* embryos do not enclose and fail to elongate. The center row shows comparable embryos stained for pharyngeal muscle to demonstrate that *efl-1;eel-1(RNAi)* embryos produce an excess of this tissue in comparison with embryos from either single mutant mother. The bottom row contains images of the MED-1:GFP expression pattern at the 15-cell stage. This expression pattern is wild-type in *eel-1(RNAi)* (*n*=25 of 25) and *efl-1(se1)* (*n*=22 of 23) single-mutant embryos; MED-1:GFP is expressed only in a subset of descendants of the posterior cell of the 2-cell embryo. In *efl-1(se1);eel-1(RNAi)* embryos (*n*=25 of 30), MED-1:GFP is ectopically expressed in descendants of the anterior blastomere of the 2-cell embryo. Embryos are oriented with anterior to the left. Scale bar: 10 μm.

Table 2. SKN-1 staining

SKN-1 level in AB(s):	Low	High	Low to intermediate	High	Absent	Present
Maternal genotype		*			**	**
20°C						
Wild type (N2)	95	5	100	0	100	0
efl-1(se1)	86	14	93	7	100	0
eel-1(zu462);efl-1(se1)	0	100	24	76	50	50
efl-1(se1);eel-1(RNAi)	0	100	38	62	74	26
eel-1(RNAi)	10	90	97	3	100	0
eel-1(zu462)/+;efl-1(se1);smg-1(RNAi)	6	94	16	84	84	16
26°C						
efl-1(se1)	13	87	0	100	92	8

Numbers indicate the percentage of embryos showing SKN-1 staining in the patterns indicated. AB is the name of the anterior blastomere of the 2-cell stage embryo, and ABs refers to its descendants at each subsequent stage. The category marked by an asterisk includes embryos with reduced SKN-1 asymmetry and loss of SKN-1 asymmetry, whereas those categories marked by two asterisks include embryos from the 12-cell stage to the 28-cell stage. Hermaphrodites were incubated at the indicated temperature. The numbers of embryos examined for each category were: at 20°C: N2 2-cell $n=22$, 4-cell $n=21$, 12-28 cell $n=35$; *efl-1(se1)* 2-cell $n=7$, 4-cell $n=14$, 12-28 cell $n=25$; *efl-1(se1);eel-1(RNAi)* 2-cell $n=18$, 4-cell $n=13$, 12-28 cell $n=54$; *eel-1(RNAi)* 2-cell $n=29$, 4-cell $n=33$, 12-28 cell $n=46$; *eel-1(zu462);efl-1(se1)* 2-cell $n=16$, 4-cell $n=21$, 12-28 cell $n=12$; *eel-1(zu462)/+;efl-1(se1);smg-1(RNAi)* 2-cell $n=18$, 4-cell $n=21$, 12-28 cell $n=12$; at 26°C: *efl-1(se1)* 2-cell $n=15$, 4-cell $n=15$, 12-28 cell $n=36$.

embryos at 20°C (Table 1). Because all mutations in this analysis confer a strict maternal effect, we will refer to the maternal genotype when describing the embryo. Thus, '*eel-1* mutant embryos' refers to embryos from *eel-1* mutant hermaphrodites.

To demonstrate that the Mex phenotype of these double-mutant embryos was caused by disruption of SKN-1 asymmetry, we first showed that the Mex phenotype was both *skn-1*-dependent [100% of *eel-1(zu462);efl-1(se1);skn-1(RNAi)* embryos were Skn; $n=107$] and *glp-1*-independent [90% of *eel-1(zu462);efl-1(se1);glp-1(RNAi)* embryos were Mex; $n=116$]. We then stained the *eel-1;efl-1* double-mutant embryos for SKN-1 and confirmed that the terminal Mex phenotype was correlated with a disruption of SKN-1 asymmetry (Table 2). Thus, the Mex phenotype of the *eel-1;efl-1* double-mutant embryos resembles the *skn-1*-dependent Mex phenotype caused by loss or reduced function of the *mex-1*, *mex-5* or *dpl-1* genes (Mello et al., 1992; Schubert et al., 2000; Page et al., 2001).

eel-1 encodes a Hect E3 ubiquitin ligase

We cloned the *eel-1* gene by a combination of traditional positional mapping, single nucleotide polymorphism (SNP) mapping and testing of candidate genes by RNAi. Our SNP mapping indicated that *eel-1* resides in a 70 kb region of chromosome IV that includes *lin-22*. We tested whether RNAi against genes in this region could enhance *efl-1(se1)* to a Mex phenotype at 20°C. RNAi of only one

gene, Y67D8C.5, enhanced *efl-1(se1)* to a Mex phenotype at 20°C (Table 1 and Fig. 1; see also Materials and methods). The *eel-1* gene, Y67D8C.5, is predicted to encode a large protein of 4,178 amino acids that exhibits strong identity with Hect ubiquitin E3 ligases.

We sequenced the Y67D8C.5 gene from the *eel-1(zu462)* background to confirm its identity as *eel-1*. In this background, the Y67D8C.5 gene contained a complicated rearrangement including a deletion and an inverted duplication (see Materials and methods). This disruption is likely to cause a C-terminal truncation in the predicted protein and a corresponding loss of the catalytic Hect ubiquitin ligase domain (Fig. 2).

The EEL-1 protein has an overall configuration similar to the mammalian E3 ligase Mule. Known in vivo targets of Mule ubiquitination include the tumor suppressor p53 (also known as Trp53), the transcription factor Myc, and the anti-apoptotic protein Mcl1 (Adhikary et al., 2005; Chen et al., 2005; Zhong et al., 2005). EEL-1 and human MULE share 70% identity in their Hect E3 catalytic domain (Fig. 2). Additionally, EEL-1 and Mule share four other domains. Two of these, DUF908 and DUF913 (domains of unknown function), are commonly found in proteins associated with the ubiquitin pathway. Both EEL-1 and Mule have a UBA (ubiquitin-binding associated) domain implicated in protein-protein interactions (Bertolaet et al., 2001; Buchberger, 2002) and a fourth domain that was not previously identified.
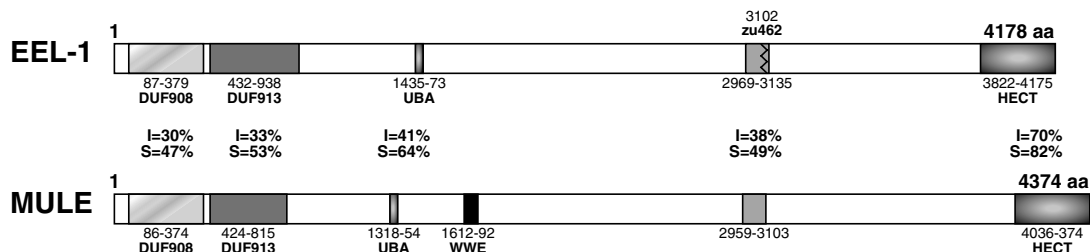
Fig. 2. Similarities between *C. elegans* EEL-1 and the human MULE E3 ligases. This diagram illustrates multiple domains shared between EEL-1 and human MULE. Between each domain of similarity, percentages of identity (I) and similarity (S) are noted. The location at which *zu462* is predicted to disrupt EEL-1 is indicated (zig-zag line).

Loss of *eel-1* reduces SKN-1 asymmetry at the 2-cell stage

Our genetic analysis of *eel-1(zu462)* indicates that it is a maternal-effect enhancer of *efl-1(se1)* (see Materials and methods). This analysis is consistent with the *eel-1* mRNA in situ pattern; *eel-1* mRNA appears enriched in the hermaphrodite gonad and is also detected at high levels in the early embryo (see the Nematode Expression Pattern Database, http://nematode.lab.nig.ac.jp/; cDNAs corresponding to *eel-1* are in cluster CELK00592). Our phenotypic analysis also suggested that the *zu462* allele is antimorphic (see data below); thus, we chose to examine in detail the reduction-of-function phenotype of *eel-1* by reducing its activity by RNAi (Fire et al., 1998). Wild-type hermaphrodites treated with *eel-1* dsRNA produced viable progeny, consistent with previous genome-wide RNAi screens (Maeda et al., 2001; Sonnichsen et al., 2005).

Terminally differentiated *eel-1(RNAi)* embryos did not have a Mex phenotype and appeared wild type with respect to both the amount of pharyngeal muscle produced and the expression pattern of the *skn-1* target construct, MED-1:GFP (Maduro et al., 2001)

(Table 1 and Fig. 1). However, the SKN-1 staining pattern in *eel-1(RNAi)* embryos was not wild-type. In 2-cell *eel-1(RNAi)* embryos, the posterior to anterior ratio of SKN-1 asymmetry appeared reduced owing to an increased level of SKN-1 in the anterior cell compared with the same cell in wild-type embryos (Fig. 3 and Table 2). By the 4-cell stage in *eel-1(RNAi)* embryos, the pattern of SKN-1 staining appeared superficially similar to wild type.

To quantitate the pattern of SKN-1 staining more precisely, we measured the amount of SKN-1 in the nucleus of each cell and determined the ratio of SKN-1 staining in the posterior cell(s) versus that in the anterior cell(s) (Fig. 4). In wild-type embryos at the 2-cell stage, this posterior to anterior ratio was 3.0 (s.e.m.±0.3; n=10), indicating that the posterior SKN-1 signal is approximately threefold brighter than the anterior signal (Fig. 4A). In wild-type embryos at the 4-cell stage, this posterior to anterior ratio increased to 4.1±0.5 (n=12), consistent with the observation by Bowerman et al. (Bowerman et al., 1993) that posterior to anterior asymmetry increases at the 4-cell stage compared with the 2-cell stage (Fig. 4B).
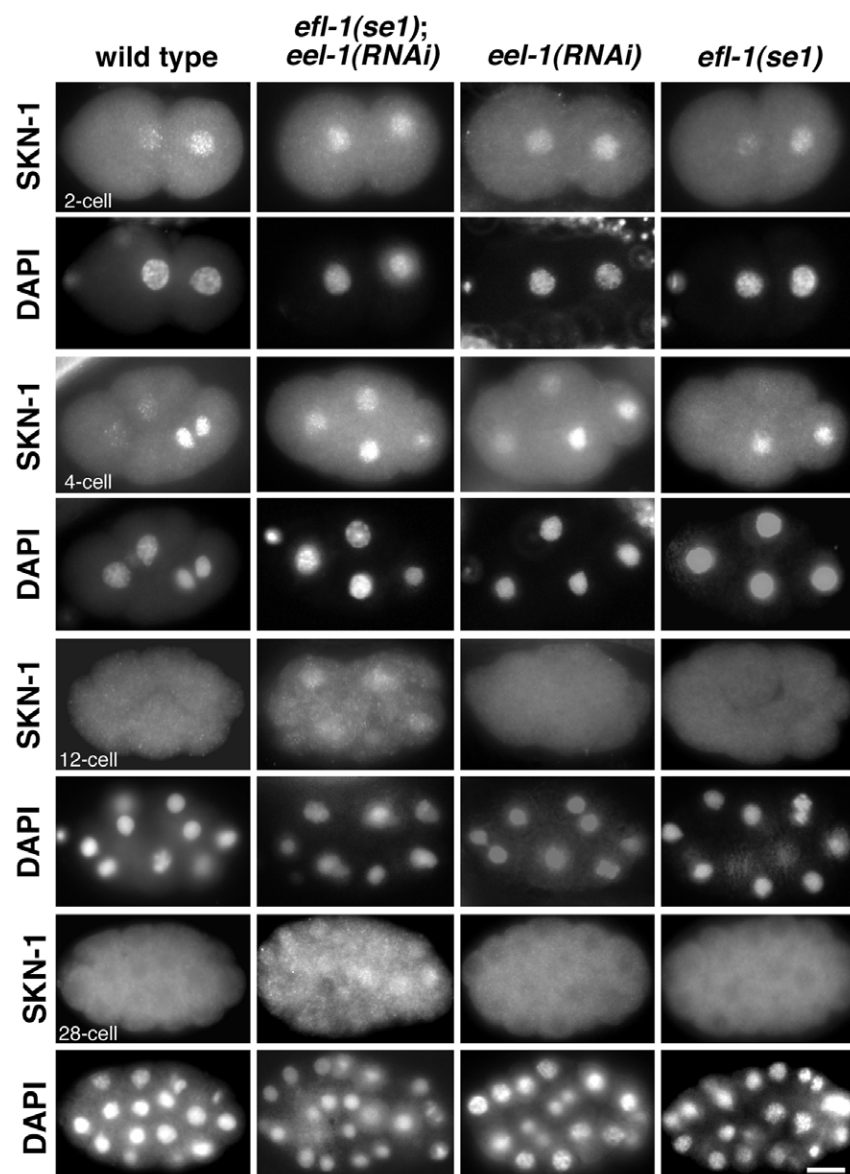
Fig. 3. Loss of *eel-1* disrupts SKN-1 spatial and temporal regulation. Each pair of rows shows SKN-1 staining (above) and corresponding nuclear staining (DAPI, below) of *C. elegans* embryos at a given stage (2-cell, 4-cell, 12-cell and 28-cell) from a hermaphrodite of indicated genotype incubated at 20°C. Embryos are oriented with anterior to the left. Scale bar: 10 μm.

DEVELOPMENT
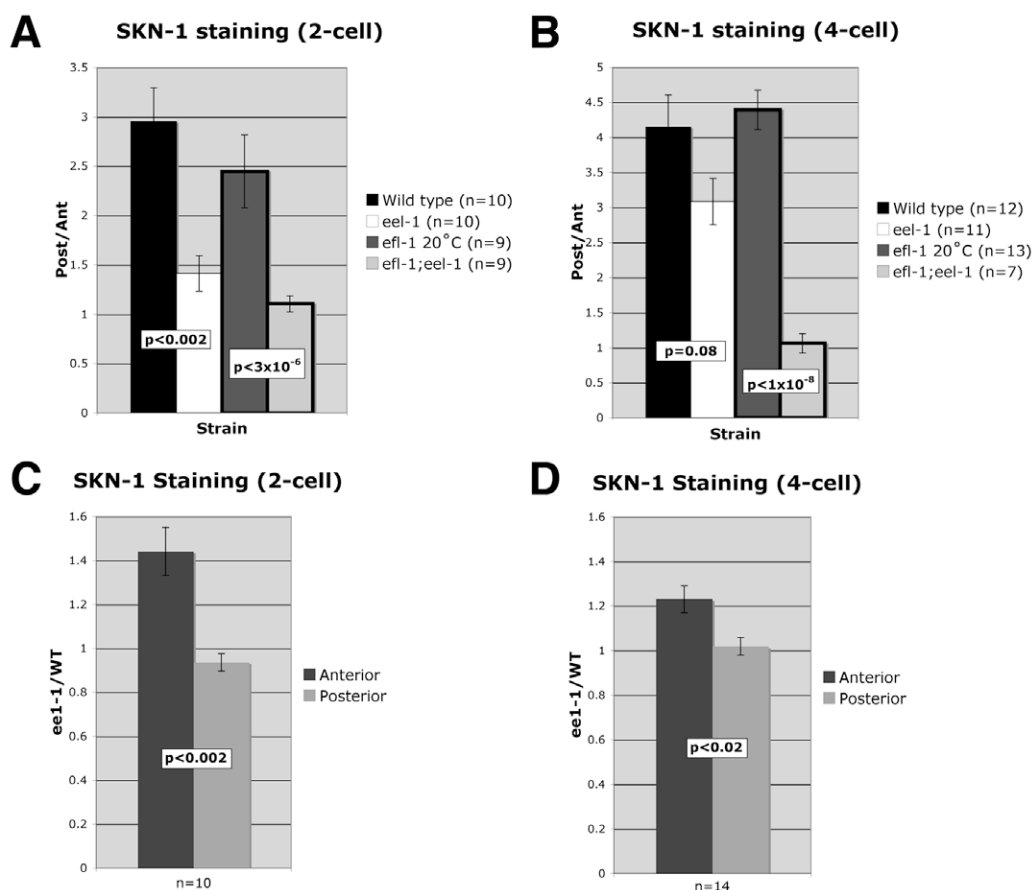
Fig. 4. SKN-1 asymmetry is disrupted in *eel-1(–)* and *efl-1(–);eel-1(–)* C. elegans embryos. (A,B) The posterior:anterior ratio (Post/Ant) of nuclear SKN-1 staining was calculated for individual embryos of the given genotype at the 2-cell (A) or 4-cell (B) stage. (C,D) Nuclear SKN-1 staining was quantitated in equivalent blastomeres for pairs of *eel-1(RNAi)* and wild-type embryos, and the *eel-1(–)* to wild-type ratio (*eel-1*/WT) was calculated for the anterior and posterior blastomere(s). Variability was minimized by performing individual comparisons between pairs of embryos from a single slide: 2-cell (C) and 4-cell (D) stage. The mean±s.e.m. is shown.

When we quantitated the level of SKN-1 staining in 2-cell embryos, we found that the posterior to anterior ratio of SKN-1 staining in *eel-1(–)* embryos (1.4±0.06; n=10) was significantly lower (P<0.002) than in wild-type embryos (3.0±0.3), indicating that the loss of *eel-1* reduces SKN-1 asymmetry at the 2-cell stage (Fig. 4A).

We then directly compared SKN-1 levels in equivalent blastomeres of wild-type and *eel-1(–)* embryos stained in the same reaction. The levels of SKN-1 in the posterior of 2-cell embryos were identical in wild-type and *eel-1(–)* embryos: the ratio of SKN-1 staining in the posterior blastomere of *eel-1(–)* embryos compared with wild-type embryos was 0.9±0.04 (n=10 pairs of embryos). Conversely, the ratio of SKN-1 staining in the anterior blastomere of *eel-1(–)* embryos compared with wild-type embryos was 1.4±0.1 (n=10 pairs of embryos) (Fig. 4C). Because the two ratios were significantly different (P<0.002), we conclude that at the 2-cell stage, loss of *eel-1* function reduces SKN-1 asymmetry by affecting SKN-1 levels specifically in the anterior blastomere.

At the 4-cell stage, SKN-1 asymmetry in *eel-1(–)* embryos appeared qualitatively more similar to that seen in wild-type embryos (Fig. 3, Fig. 4 and Table 2). Quantitation of the posterior:anterior SKN-1 ratio in 4-cell *eel-1(–)* embryos (3.1±0.3; n=11) indicated that this ratio was not significantly different (P=0.08) from that of wild-type embryos (4.1±0.5).

However, direct comparison of the levels of SKN-1 staining between wild-type and *eel-1(–)* 4-cell embryos revealed a small but significant effect on SKN-1 asymmetry (Fig. 4D). The levels of SKN-1 in the posterior of the 4-cell embryo were identical between wild-type and *eel-1(–)* embryos: the ratio of SKN-1 staining in the posterior blastomeres of 4-cell *eel-1(–)* embryos compared with wild-type embryos was 1.0±0.06 (n=14 pairs of embryos). Conversely, the ratio of SKN-1 staining in the anterior blastomeres of 4-cell *eel-1(–)* embryos compared with wild-type embryos was 1.2±0.04 (n=14 pairs of embryos). The difference between these ratios was small but statistically significant (P<0.02), indicating that loss of *eel-1* also affected SKN-1 asymmetry at the 4-cell stage.

Taken together, these data indicate that loss of *eel-1* function perturbs SKN-1 asymmetry at the 2-cell stage, and has a small but significant effect on SKN-1 asymmetry at the 4-cell stage. By the 12-cell stage, SKN-1 protein was no longer detected in either wild-type or *eel-1(RNAi)* embryos (Fig. 3).

eel-1 acts redundantly with *efl-1* to control SKN-1 spatial asymmetry and temporal perdurance

As previously described, *efl-1(se1)* embryos were viable at 20°C and appeared wild type with respect to both the amount of pharyngeal muscle produced and MED-1:GFP expression (Fig. 1). Quantitation

of the levels of SKN-1 expression in *efl-1(se1)* embryos confirmed that the pattern of SKN-1 asymmetry was not statistically different from that of wild type. In 2-cell *efl-1(se1)* embryos, the posterior:anterior ratio of SKN-1 expression was 2.4±0.1 (*n*=9) compared with the wild-type value of 3.0±0.3 (*P*=0.18). In 4-cell *efl-1(se1)* embryos, the ratio was 4.4±0.3 (*n*=13), compared with the wild-type value of 4.1±0.5 (*P*=0.77) (Fig. 4A).

Reduction of *eel-1* by RNAi in an *efl-1(se1)* background produced a dramatic effect: 85% of *efl-1(se1);eel-1(RNAi)* embryos died with a Mex phenotype (Table 1 and Fig. 1). Like the Mex phenotype of *efl-1(se1);eel-1(zu462)* embryos, the Mex phenotype of *efl-1(se1);eel-1(RNAi)* embryos was also dependent on *skn-1* function; all *efl-1(se1);eel-1(RNAi);skn-1(RNAi)* triple-mutant embryos were Skn in terminal phenotype (*n*=168). Consistent with this *skn-1*-dependent Mex phenotype, MED-1:GFP was expressed ectopically in *efl-1(se1);eel-1(RNAi)* embryos (Fig. 1). This ectopic MED-1:GFP expression occurred in the descendants of the anterior blastomere of the 2-cell embryo, and this expression pattern appeared identical to that seen in *mex-1* and *mex-5* mutant embryos (Maduro et al., 2001; Tenlen et al., 2006).

When we stained for SKN-1 we found that, as expected, *efl-1(se1);eel-1(RNAi)* embryos showed a qualitative disruption in SKN-1 asymmetry. High levels of SKN-1 were detected in the anterior cell at the 2-cell stage and in this cell's daughters at the 4-cell stage (Fig. 3 and Table 2). Quantitation of SKN-1 staining in these *efl-1;eel-1* double-mutant embryos revealed an almost complete loss of asymmetry (Fig. 4A,B). At the 2-cell stage, the posterior:anterior ratio was 1.1±0.03 [*n*=9; $P<3\times10^{-6}$ compared with the posterior:anterior ratio of *efl-1(se1)* embryos], and at the 4-cell stage this ratio was 1.0±0.1 [*n*=7; $P<1\times10^{-8}$ compared with *efl-1(se1)* embryos]. Thus, there is a profound enhancement of each single-mutant phenotype. This enhancement indicates that the two genes act in functionally redundant pathways to affect SKN-1 asymmetry.

The functional genetic redundancy between *efl-1(se1)* and *eel-1(−)* was not limited to an effect on SKN-1 asymmetry. Slightly older *efl-1(se1);eel-1(RNAi)* embryos showed an unusual SKN-1 pattern. In early embryos from wild-type and *efl-1(se1)* mothers incubated at 20°C, SKN-1 disappears after the 8-cell stage (Bowerman et al., 1993) (Table 2). By contrast, in *efl-1(se1);eel-1(−)* mutant embryos, SKN-1 could be detected in all cells up to the 28-cell stage (Fig. 3 and Table 2). Thus, in the *efl-1(se1)* background, loss of *eel-1* not only completely disrupts SKN-1 asymmetry at the 2- and 4-cell stages, but also causes the SKN-1 protein to persist in the descendants of both the anterior and posterior blastomeres.
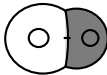
Loss of *eel-1* appears to affect SKN-1 specifically

Aberrant expression of SKN-1 in *eel-1(−)* embryos could be due to a direct effect of EEL-1 on SKN-1. Alternatively, EEL-1 could perturb SKN-1 expression indirectly, as a consequence of the effect of EEL-1 on global anterior/posterior (A/P) polarity. Because several A/P polarity mutants have defects in asymmetry of at least two of the following three proteins, PIE-1, PGL-1 and MEX-5 (Rose and Kemphues, 1998; Tenenhaus et al., 1998; Schubert et al., 2000; Lin, 2003; DeRenzo and Seydoux, 2004; Shirayama et al., 2006), we explored the specificity of EEL-1 action by examining the expression pattern of these proteins in *eel-1(RNAi)* embryos. PIE-1 is a nuclear and cytoplasmic protein containing two CCCH zinc-finger domains (Mello et al., 1996), and PGL-1 is a component of P granules, which are cytoplasmic structures

enriched in germ plasm (Kawasaki et al., 1998). At the 2-cell stage, both PIE-1 and PGL-1 are localized to the posterior cell that is the progenitor of germline, and both are enriched in the germline progenitor at each subsequent cell division (Mello et al., 1996; Kawasaki et al., 1998; Tenenhaus et al., 1998). MEX-5 is present in the anterior blastomere at the 2-cell stage and becomes enriched in the somatic daughter of the germline progenitor at each successive division of the germline lineage (Schubert et al., 2000). In 2- and 4-cell *eel-1(RNAi)* embryos, and in 2- and 4-cell *efl-1(se1)* embryos at 20°C, the pattern of PIE-1, PGL-1 and MEX-5 expression appeared wild-type (Table 3). Removal of *eel-1* function in the *efl-1(se1)* background did not disrupt the asymmetry of PIE-1, PGL-1 or MEX-5 in 2- or 4-cell embryos (Table 3). The wild-type pattern of multiple, asymmetrically expressed proteins in *eel-1(RNAi)* embryos suggests that the action of EEL-1 is specific to SKN-1.

To further investigate the specificity of EEL-1 embryonic function, we took a genetic approach. As described above, mutations in four genes, *mex-5*, *mex-1*, *dpl-1* and *efl-1*, can cause misexpression of SKN-1 at the 2-cell stage and these terminally developed mutant embryos contain an excess of *skn-1*-dependent pharyngeal tissue (Mello et al., 1992; Schubert et al., 2000; Page et al., 2001). In addition to SKN-1 asymmetry, each of the above mutants affects other aspects of A/P polarity. This latter effect is most easily seen by examining the phenotype of certain double mutants between the above Mex genes or between one of these Mex genes and *mex-6*, a gene that encodes a protein with 85% similarity to MEX-5. In contrast to the Mex phenotype, these double-mutant embryos lack pharyngeal tissue (Schubert et al., 2000; Page et al., 2001; Huang et al., 2002). This phenotype, called Skn, is associated with, and is caused by, a severe disruption in the asymmetry of multiple proteins (Schubert et al., 2000; Page et al., 2001; Huang et al., 2002). Although SKN-1 is misexpressed in these embryos, it is not active owing to the concomitant mislocalization of a protein that negatively regulates SKN-1 activity. Thus, these embryos have a terminal phenotype that is superficially similar to that caused by lack of *skn-1(+)* activity. This genetic assay appears to be very sensitive, as loss of *mex-6* results in viable embryos that show asymmetry of all early embryonic markers examined, including SKN-1 (Schubert et al., 2000). Like *efl-1;eel-1* double-mutant embryos, *efl-1(se1);mex-6(−)* embryos were Mex at 20°C, but *mex-5;mex-6* mutant embryos are Skn (Table 4) (Schubert et al., 2000).

Table 3. *eel-1(RNAi)* does not affect the asymmetric expression of other proteins

Maternal genotype	PIE-1	PGL-1	MEX-5
Wild type (N2)	100 (*n*=19)	100 (*n*=19)	100 (*n*=32)
eel-1(RNAi)	100 (*n*=23)	100 (*n*=13)	100 (*n*=13)
efl-1(se1)	100 (*n*=35)	100 (*n*=25)	100 (*n*=25)
efl-1(se1);eel-1(RNAi)	100 (*n*=26)	100 (*n*=10)	100 (*n*=25)

Numbers indicate the percentage (all 100%) of embryos expressing PIE-1, PGL-1 and MEX-5 in the indicated asymmetric pattern observed in wild-type embryos. All hermaphrodites were incubated at 20°C, the permissive temperature for *efl-1(se1)*. Similar experiments were also carried out on 4-cell embryos: wild type: PIE-1, *n*=32; PGL-1, *n*=15; MEX-5, *n*=23. *eel-1(RNAi)*: PIE-1, *n*=30; PGL-1, *n*=7; MEX-5, *n*=9. *efl-1(se1)*: PIE-1, *n*=31; PGL-1, *n*=19; MEX-5, *n*=28. *efl-1;eel-1(RNAi)*: PIE-1, *n*=16; PGL-1, *n*=10; MEX-5, *n*=18.

Table 4. Loss of *eel-1* does not enhance the terminal phenotype of other *skn-1*-dependent Mex mutants

Maternal genotype	Phenotype	%	*n*
Wild type (N2)	Wild type	99	310
efl-1(se1)	Wild type	88	207
eel-1(RNAi)	Wild type	98	177
efl-1(se1);eel-1(RNAi)	Mex	90	60
dpl-1(zu355)	Mex	86	114
dpl-1(zu355);mex-5(RNAi)	Skn	82	50
dpl-1(zu355);eel-1(RNAi)	Mex	99	140
mex-5(RNAi)	Mex	96	68
efl-1(se1);mex-5(RNAi)	Skn	92	60
mex-5(zu199)	Mex	100	119
mex-5(zu199);mex-6(RNAi)	Skn	100	109
mex-5(zu199);mex-1(RNAi)	Skn	97	139
mex-5(zu199);eel-1(RNAi)	Mex	100	279
mex-1(RNAi)	Mex	99	157
efl-1(se1);mex-1(RNAi)	Mex	99	137
mex-1(zu120)	Mex	100	135
mex-1(zu120);mex-6(RNAi)	Mex	100	107
mex-1(zu120);eel-1(RNAi)	Mex	99	102
mex-6(RNAi)	Wild type	100	96
efl-1(se1);mex-6(RNAi)	Mex	92	84
mex-6(pk440);eel-1(RNAi)	Wild type	93	105

All hermaphrodites were incubated at 20°C. These terminal Mex mutant embryos have an excess of pharyngeal muscle cells. The terminal Skn phenotype refers to a loss of pharyngeal muscle.

We reasoned that if *eel-1(–)* affects general A/P polarity in addition to SKN-1 asymmetry, then loss of *eel-1* in combination with other Mex mutants would result in the more severe Skn phenotype; however, if *eel-1(–)* does not enhance the phenotype of these Mex mutants, EEL-1 is likely to be affecting SKN-1 specifically. Our detailed analysis of these interactions showed that the *mex-5(–)* background is the most sensitive to such enhancement. The combination of either *efl-1(–)*, *mex-6(–)*, *dpl-1(–)* or *mex-1(–)* mutants with *mex-5(–)* resulted in the majority of embryos having the severe Skn phenotype; however, loss of *eel-1* in the background of *mex-5(–)* did not alter the *mex-5(–)* terminal phenotype (Table 4). In fact, *eel-1(–)* in combination with any of these Mex mutants did not result in a Skn phenotype, and the *mex-6(–);eel-1(–)* double mutant hermaphrodites laid viable embryos. Additionally, embryos from *efl-1(se1);eel-1(RNAi)* mothers incubated at 26°C [the *efl-1(se1)* restrictive temperature] were Mex, not Skn (100% Mex, *n*=112). This genetic analysis shows that removal of *eel-1* in the background of multiple Mex mutants does not alter their terminal phenotype. These data strongly support the hypothesis that, unlike the Mex genes that control multiple aspects of A/P polarity including SKN-1 asymmetry, *eel-1* specifically affects SKN-1 accumulation.

The *eel-1(zu462)* allele encodes a dominant-negative protein

In examining the effect of *eel-1(zu462)* on *efl-1(se1)*, we noticed that *efl-1(se1)* hermaphrodites heterozygous for *eel-1(zu462)* generated a higher percentage of Mex embryos than *efl-1(se1)* controls (24% versus 0% Mex, respectively, Table 1). Although this phenomenon could be due to haplo-insufficiency, our molecular analysis of *eel-1(zu462)* led us to consider an alternative hypothesis. The truncated *eel-1(zu462)* message might create an EEL-1 protein with a

dominant-negative function. Since the nonsense-mediated mRNA decay pathway acts to eliminate aberrant messages (Pulak and Anderson, 1993), the *zu462* message is probably unstable. If the truncated protein encoded by the *zu462* message is dominant-negative, then increasing the stability of the *zu462* mRNA should increase the penetrance of the Mex phenotype in embryos from *eel-1(zu462)/(+);efl-1(se1)* mothers. To test this, we used RNAi to reduce the function of *smg-1*, a member of the nonsense-mediated mRNA decay pathway (Pulak and Anderson, 1993). Treatment of *eel-1(zu462)/(+);efl-1(se1)* hermaphrodites with *smg-1* dsRNA increased the percentage of Mex embryos from 24% to 90% (Table 1), and a high percentage (94% 2-cell; 86% 4-cell) of these embryos showed a disruption in SKN-1 asymmetry (Table 2). These data indicate that stabilizing the *eel-1(zu462)* mRNA results in a dominant-negative EEL-1 protein.

The EEL-1 truncation is predicted to lack the catalytic Hect E3 ubiquitin ligase domain, but would contain the DUF908, DUF913 and UBA domains as well as a fourth novel domain (Fig. 2). UBA domains have been implicated in binding ubiquitin and in protein-protein interactions (Bertolaet et al., 2001; Buchberger, 2002). Thus, the EEL-1(dominant-negative) protein still could bind member(s) of the ubiquitin pathway but be unable to perform its catalytic function.

The N-terminus of EEL-1 interacts with the C-terminus of SKN-1

As a predicted Hect E3 ligase, EEL-1 has two likely interaction partners – its E2 conjugating enzyme and its target (Pickart, 2001; Kipreos, 2005). Because our analysis suggested that SKN-1 might be the target of EEL-1, we used the yeast two-hybrid assay to test whether EEL-1 interacts with SKN-1. We tested two regions of EEL-1 for interaction with SKN-1: an N-terminal region (975-2018 aa) and the C-terminus (3429-4177 aa). Indicative of an interaction between SKN-1 and the N-terminus of EEL-1, yeast containing both the EEL-1 N-terminal fusion and the SKN-1 fusion grew on selective media, whereas yeast containing both the EEL-1 C-terminal fusion and the SKN-1 fusion did not (Fig. 5A). The corresponding negative controls did not grow on selective media (Fig. 5A).

To define further the interaction domain for each protein, we tested smaller regions of EEL-1 and SKN-1 (Fig. 5A). EEL-1(1307-2018 aa) interacted with SKN-1(298-623 aa); no interaction was detected for controls (Fig. 5A,B). Amino acids 1307-2018 of EEL-1 encompass the UBA domain, and the 298-623 aa region of SKN-1 includes the DNA-binding domain and a nuclear localization signal. To rule out the possibility that EEL-1(975-2018 aa) indiscriminately associates with nuclear proteins, we tested whether it could interact with three yeast nuclear proteins, SIR3, SIR4 and SNF4. No interaction was detected between any of these proteins and EEL-1 (not shown). Thus, EEL-1 interacts with the C-terminus of SKN-1.

The C-terminus of SKN-1 can target GFP for degradation in a temporal pattern that is EEL-1-dependent

To determine whether the C-terminus of SKN-1 could affect protein stability and whether this stability could be controlled by *eel-1*, we fused the part of *skn-1* encoding amino acids 298 to 623 to the coding region of *gfp*. We placed this GFP:SKN-1(298-623) fusion under control of the *pie-1* promoter and the *pie-1* 3′UTR. This system had been shown to give robust embryonic expression of multiple genes (Strome et al., 2001) and, in fact, this was the only vector we tried that gave early embryonic expression of chimeric SKN-1 protein. Furthermore, we reasoned that by using the *pie-1* 3′UTR instead of

A

| EEL-1	SKN-1	interaction
975-2018	37-623	+
975-2018	37-244	-
975-2018	298-623	+++
975-2018	vector	-
vector	37-623	-
vector	298-623	-
975-1373	298-623	-
1307-2018	37-623	+
1307-2018	298-623	+++
1307-2018	37-244	-
1307-2018	vector	-
3429-4177	37-623	-
vector	vector	-
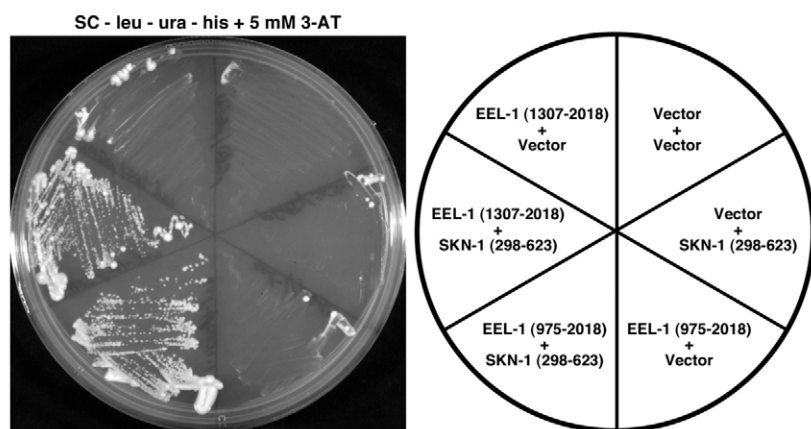
Fig. 5. EEL-1 interacts with SKN-1 in the yeast two-hybrid assay. (**A**) The level of two-hybrid interactions between *C. elegans* EEL-1 and SKN-1. The left column indicates the amino acids of EEL-1 fused to the GAL4 DNA-binding domain, and the central column indicates the amino acids of SKN-1 fused to the GAL4 activation domain. The domain structure of EEL-1 is shown in Fig. 2. SKN-1 has 623 amino acid residues, and its DNA-binding domain comprises residues 549-614. The right column shows the level of growth on selective medium when yeast are transformed with the corresponding plasmids. (**B**) Two-hybrid interaction between EEL-1 and SKN-1.

B

SC - leu - ura - his + 5 mM 3-AT

EEL-1 (1307-2018) + Vector

Vector + Vector

Vector + SKN-1 (298-623)

EEL-1 (1307-2018) + SKN-1 (298-623)

EEL-1 (975-2018) + SKN-1 (298-623)

EEL-1 (975-2018) + Vector

the *skn-1* 3′UTR, we reduced the chance that we were examining an effect of *eel-1(–)* upon factors that bind the *skn-1* 3′UTR. One limitation of this vector, however, is that it gives robust protein expression in the maternal germline (Strome et al., 2001). This expression pattern contrasts with that of the endogenous SKN-1, a protein that is not detected until after fertilization (Bowerman et al., 1993). The large amount of germline-produced protein thus prevented us from determining whether the SKN-1(298-623) domain could be spatially regulated in a manner similar to that of endogenous SKN-1.

Despite this limitation of the *pie-1* expression vector, we were able to evaluate the temporal regulation of the GFP:SKN-1 fusion. As expected, we saw strong GFP expression in the oocytes of hermaphrodites carrying either the GFP vector control or the GFP:SKN-1 fusion. Embryos expressing the control vector encoding only GFP showed a strong signal in all nuclei from the 1- to 28-cell stage (*n*=48, 15-cell stage; *n*=46, 28-cell stage) (Fig. 6). Embryos expressing the GFP:SKN-1(298-623) fusion also showed a strong nuclear signal in 1- to 6-cell embryos. However, by the 8-cell stage, the GFP:SKN-1(298-623) signal was greatly reduced in comparison with its signal in earlier embryos and to the signal detected for GFP alone (not shown). By the 15-cell stage, GFP:SKN-1(298-623) was seen in only 12% of embryos (*n*=32) (Fig. 6), and at the 28-cell stage none of the embryos had a detectable GFP:SKN-1 signal (*n*=30). This temporal pattern of the GFP:SKN-1(298-623) signal is similar to that of endogenous SKN-1 in wild-type embryos (Bowerman et al., 1993).

Since the temporal pattern of the GFP:SKN-1(298-623) fusion shared similarity to that of endogenous SKN-1, we tested whether removing *eel-1* by RNAi could alter the stability of this fusion. In contrast to the disappearance of GFP:SKN-1(298-623) in wild-type embryos, the GFP:SKN-1(298-623) signal persisted in *eel-1(RNAi)* embryos. At the 15-cell stage, 92% of *eel-1(RNAi)* embryos showed a strong GFP:SKN-1(298-623) signal in all nuclei (*n*=48) (Fig. 6). This GFP:SKN-1(298-623) signal persisted in the *eel-1(RNAi)* embryos to the 28-cell stage (100%, *n*=35), but was greatly reduced thereafter (not shown). Removal of *eel-1* did not affect the

wild type   *eel-1(RNAi)*

GFP
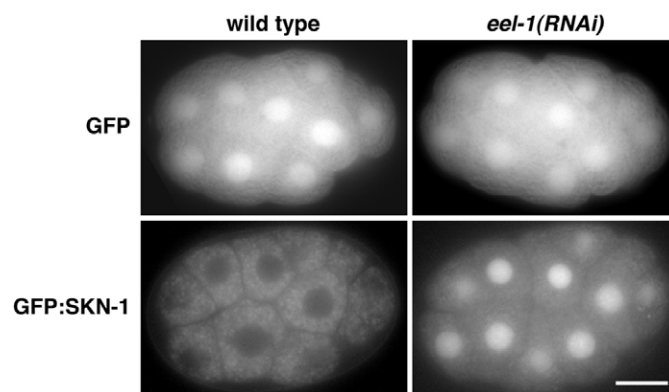
GFP:SKN-1

Fig. 6. The C-terminus of SKN-1 targets GFP for degradation in an EEL-1-dependent manner. Wild-type (left) and *eel-1(RNAi)* (right) 15-cell *C. elegans* embryos expressing GFP (top row) or GFP:SKN-1(298-623) fusion protein (bottom row) under control of the *pie-1* promoter and *pie-1* 3′UTR. Embryos are oriented with anterior to the left. Scale bar: 10 μm.

expression pattern or level of GFP in embryos expressing the control vector (*n*=43 for 15-cell stage and *n*=47 for 28-cell stage, Fig. 6). The temporal pattern of the GFP:SKN-1 fusion in wild-type and *eel-1(RNAi)* embryos was thus very similar to the pattern of endogenous SKN-1 in *efl-1(se1)* and *efl-1(se1);eel-1(RNAi)* embryos, respectively. These experiments demonstrate that the C-terminus of SKN-1 can target a protein for degradation in a temporal pattern similar to that of endogenous SKN-1 and that this degradation is dependent on *eel-1*.

DISCUSSION
EEL-1, an E3 ubiquitin ligase, regulates the spatial distribution and temporal stability of SKN-1
We have characterized the putative Hect E3 protein ligase EEL-1 and identified SKN-1 as a potential EEL-1 substrate. We propose that *eel-1* is one of multiple genes that act together to control both the asymmetric accumulation and the temporal stability of SKN-1 in the early *C. elegans* embryo.

The *eel-1* mutation is an enhancer of the *efl-1(se1)* mutation at its permissive temperature. At this temperature, embryos from *efl-1(se1)* hermaphrodites have an essentially wild-type pattern of SKN-1 and develop normally, whereas embryos from *efl-1;eel-1* double-mutant hermaphrodites die with a terminal Mex phenotype. Although it dramatically enhances the phenotype of *efl-1(se1)* embryos, loss of *eel-1* activity alone confers only a subtle phenotype. In embryos from *eel-1(–)* hermaphrodites, the spatial asymmetry of SKN-1 is reduced at the 2-cell stage. However, SKN-1 asymmetry is largely restored by the 4-cell stage, and endogenous SKN-1 protein is eliminated at its normal time. Since SKN-1 does not activate transcription until the 4-cell stage (Robertson et al., 2004), ectopic SKN-1 present at the 2-cell stage does not disrupt normal development, and *eel-1* mutant embryos hatch without an obvious phenotype.

We cloned *eel-1* and showed that it encodes a protein with strong homology to the family of Hect E3 ubiquitin protein ligases. This class of proteins acts to transfer ubiquitin domains to their substrates, usually targeting the substrate for proteasome-mediated destruction (Pickart, 2001). EEL-1 could affect SKN-1 expression directly, or indirectly through proteins required for A/P polarity. To distinguish between these possibilities, we first examined the patterns of three other asymmetrically expressed proteins, PIE-1, PGL-1 and MEX-5, in *eel-1(–)* embryos. The expression patterns of these proteins, as well as SKN-1, are disrupted in many mutants defective in multiple aspects of A/P polarity, such as *mex-5/6*, *mex-1*, *oma-1* and the *par* mutants (Bowerman et al., 1993; Guedes and Priess, 1997; Rose and Kemphues, 1998; Tenenhaus et al., 1998; Schubert et al., 2000; Lin, 2003; DeRenzo and Seydoux, 2004; Shirayama et al., 2006). We found that the asymmetry of PIE-1, PGL-1 and MEX-5 appears normal in *eel-1(–)* embryos. Moreover, we demonstrated that *eel-1(–)* does not enhance any *skn-1*-dependent Mex mutant to a more severe Skn terminal phenotype. These data, combined with the observation that the defects in SKN-1 accumulation in *eel-1* mutants are different from those in any known A/P polarity mutant, strongly suggest that loss of *eel-1* is not indirectly affecting SKN-1 by causing a general defect in A/P polarity.

Instead, our data are compatible with the hypothesis that SKN-1 is a direct target of EEL-1. First, the asymmetry of SKN-1 is selectively reduced in the *eel-1(–)* background, and, in the *efl-1(–);eel-1(–)* background, SKN-1 is the only known protein whose asymmetry is abolished. Second, EEL-1 can specifically bind the C-terminus of SKN-1 in a yeast two-hybrid assay. Third, the temporal degradation of a fusion protein containing the

C-terminal region of SKN-1 is dependent on EEL-1 activity. EEL-1 is the first HECT-domain ubiquitin ligase that has been implicated in controlling asymmetric protein expression in the 2-cell embryo.

The closest ortholog of EEL-1 is the mammalian E3 ligase Mule. EEL-1 and Mule share five domains, and these domains are similarly positioned in both proteins. Mule has been demonstrated to ubiquitinate three proteins – the tumor suppressor p53, the Myc oncogene and the anti-apoptotic factor Mcl1. In the case of p53 and Mcl1, ubiquitination by Mule targets these proteins for degradation (Chen et al., 2005; Zhong et al., 2005). However, Mule ubiquitination of Myc is positively correlated with Myc's function as a transcriptional activator (Adhikary et al., 2005). Our genetic data indicate that EEL-1 promotes SKN-1 degradation, as removal of *eel-1* in two backgrounds causes an increase in SKN-1 levels and/or activity. However, SKN-1 is unlikely to be the only substrate of EEL-1.

EEL-1 acts redundantly with one or more EFL-1 targets to regulate SKN-1 accumulation spatially and temporally
We have shown that *eel-1(–)* embryos have a significant reduction in the spatial asymmetry of SKN-1 at the 2-cell stage, and a small reduction in spatial asymmetry of SKN-1 at the 4-cell stage. This reduction in spatial asymmetry results from an increase of SKN-1 in the anterior blastomere(s). These data indicate that EEL-1 promotes the strong SKN-1 asymmetry at the 2-cell stage.

When we examined the pattern of SKN-1 expression in *efl-1;eel-1* double-mutant embryos, we found that EEL-1 is functionally redundant with processes controlled by the EFL-1 transcription factor. Specifically in *efl-1;eel-1* double mutants, SKN-1 asymmetry is completely abolished at the 2- and 4-cell stages. Additionally, in these double-mutant embryos the temporal pattern of SKN-1 elimination is disrupted. Whereas SKN-1 disappears immediately after the 8-cell stage in each single mutant, in the double-mutant embryos SKN-1 could be detected in all cells until the 28-cell stage. Thus, EEL-1 function is partially redundant with EFL-1 activity in controlling SKN-1 asymmetry at the 2- and 4-cell stages. Later, EEL-1 and EFL-1 function redundantly in a spatially non-restricted fashion to control SKN-1 persistence during the 12- to 28-cell stages.

The role of *eel-1* in controlling the temporal regulation of SKN-1 was also demonstrated by comparing the expression pattern of a GFP:SKN-1 fusion protein in wild-type and *eel-1(–)* embryos. Specifically, whereas the fusion protein is degraded by the 15-cell stage in otherwise wild-type embryos, the GFP:SKN-1 can persist until the 28-cell stage in *eel-1(–)* embryos. Because the degradation of the GFP:SKN-1 fusion is regulated by *eel-1* independently of the action of *efl-1*, we propose that the temporal control of SKN-1 by the *efl-1*-dependent mechanism is through a portion of *skn-1(+)* not included in the GFP:SKN-1 fusion construct – either a domain of the protein or the 3′UTR of the *skn-1* mRNA.

How can we reconcile the apparent spatial specificity of EEL-1 action at the 2- and 4-cell stage with its apparent uniform activity slightly later during embryogenesis? There are two possible scenarios. First, the spatial accumulation of EEL-1 protein could be complementary to that of SKN-1 during the 2- and 4-cell stages, but be uniform during later stages. Alternatively, EEL-1 could be uniformly expressed, but the action of EEL-1 on SKN-1 could be regulated by spatially specific post-translational modifications of either EEL-1 or SKN-1 during early cell stages. There are multiple examples in which the activity of either an E3 ligase or its substrate

is regulated post-translationally (Laney and Hochstrasser, 1999). For example, the E3 ligase activity of EEL-1 could be controlled by phosphorylation, as in case of the Hect E3 ligase Itch (Gao et al., 2004). Alternatively, ubiquitin-dependent degradation of a protein can be enhanced or suppressed by its phosphorylation (Musti et al., 1997; Deng et al., 2004; Eckerdt et al., 2005; Nishi and Lin, 2005; Stitzel et al., 2006). Either of these hypotheses could explain spatially restricted activity at one stage, but uniform activity at a slightly later stage. Further work is necessary to establish the mechanisms controlling the spatial and temporal dynamics of the EEL-1–SKN-1 interaction.

References

Adhikary, S., Marinoni, F., Hock, A., Hulleman, E., Popov, N., Beier, R., Bernard, S., Quarto, M., Capra, M., Goettig, S. et al. (2005). The ubiquitin ligase HectH9 regulates transcriptional activation by Myc and is essential for tumor cell proliferation. *Cell* **123**, 409-421.

Bertolaet, B. L., Clarke, D. J., Wolff, M., Watson, M. H., Henze, M., Divita, G. and Reed, S. I. (2001). UBA domains mediate protein-protein interactions between two DNA damage-inducible proteins. *J. Mol. Biol.* **313**, 955-963.

Bowerman, B. (2000). Embryonic polarity: protein stability in asymmetric cell division. *Curr. Biol.* **10**, R637-R641.

Bowerman, B., Eaton, B. A. and Priess, J. R. (1992). skn-1, a maternally expressed gene required to specify the fate of ventral blastomeres in the early C. elegans embryo. *Cell* **68**, 1061-1075.

Bowerman, B., Draper, B. W., Mello, C. C. and Priess, J. R. (1993). The maternal gene skn-1 encodes a protein that is distributed unequally in early C. elegans embryos. *Cell* **74**, 443-452.

Brenner, S. (1974). The genetics of Caenorhabditis elegans. *Genetics* **77**, 71-94.

Buchberger, A. (2002). From UBA to UBX: new words in the ubiquitin vocabulary. *Trends Cell Biol.* **12**, 216-221.

Chen, D., Kon, N., Li, M., Zhang, W., Qin, J. and Gu, W. (2005). ARF-BP1/Mule is a critical mediator of the ARF tumor suppressor. *Cell* **121**, 1071-1083.

Chi, W. and Reinke, V. (2006). Promotion of oogenesis and embryogenesis in the C. elegans gonad by EFL-1/DPL-1 (E2F) does not require LIN-35 (pRB). *Development* **133**, 3147-3157.

Deng, X., Mercer, S. E., Shah, S., Ewton, D. Z. and Friedman, E. (2004). The cyclin-dependent kinase inhibitor p27Kip1 is stabilized in G(0) by Mirk/dyrk1B kinase. *J. Biol. Chem.* **279**, 22498-22504.

DeRenzo, C. and Seydoux, G. (2004). A clean start: degradation of maternal proteins at the oocyte-to-embryo transition. *Trends Cell Biol.* **14**, 420-426.

DeRenzo, C., Reese, K. J. and Seydoux, G. (2003). Exclusion of germ plasm proteins from somatic lineages by cullin-dependent degradation. *Nature* **424**, 685-689.

Doe, C. Q. and Bowerman, B. (2001). Asymmetric cell division: fly neuroblast meets worm zygote. *Curr. Opin. Cell Biol.* **13**, 68-75.

Eckerdt, F., Yuan, J., Saxena, K., Martin, B., Kappel, S., Lindenau, C., Kramer, A., Naumann, S., Daum, S., Fischer, G. et al. (2005). Polo-like kinase 1-mediated phosphorylation stabilizes Pin1 by inhibiting its ubiquitination in human cells. *J. Biol. Chem.* **280**, 36575-36583.

Evans, T. C., Crittenden, S. L., Kodoyianni, V. and Kimble, J. (1994). Translational control of maternal glp-1 mRNA establishes an asymmetry in the C. elegans embryo. *Cell* **77**, 183-194.

Fire, A., Xu, S., Montgomery, M. K., Kostas, S. A., Driver, S. E. and Mello, C. C. (1998). Potent and specific genetic interference by double-stranded RNA in Caenorhabditis elegans. *Nature* **391**, 806-811.

Gao, M., Labuda, T., Xia, Y., Gallagher, E., Fang, D., Liu, Y. C. and Karin, M. (2004). Jun turnover is controlled through JNK-dependent phosphorylation of the E3 ligase Itch. *Science* **306**, 271-275.

Guedes, S. and Priess, J. R. (1997). The C. elegans MEX-1 protein is present in germline blastomeres and is a P granule component. *Development* **124**, 731-739.

Huang, N. N., Mootz, D. E., Walhout, A. J., Vidal, M. and Hunter, C. P. (2002).

MEX-3 interacting proteins link cell polarity to asymmetric gene expression in Caenorhabditis elegans. *Development* **129**, 747-759.

Kamath, R. S. and Ahringer, J. (2003). Genome-wide RNAi screening in Caenorhabditis elegans. *Methods* **30**, 313-321.

Kawasaki, I., Shim, Y. H., Kirchner, J., Kaminker, J., Wood, W. B. and Strome, S. (1998). PGL-1, a predicted RNA-binding component of germ granules, is essential for fertility in C. elegans. *Cell* **94**, 635-645.

Kipreos, E. T. (2005). Ubiquitin-mediated pathways in C. elegans. In *WormBook* (ed. The *C. elegans* Research Community), doi:10.1895/wormbook.1.36.1, http://www.wormbook.org.

Lai, W. S., Carballo, E., Strum, J. R., Kennington, E. A., Phillips, R. S. and Blackshear, P. J. (1999). Evidence that tristetraprolin binds to AU-rich elements and promotes the deadenylation and destabilization of tumor necrosis factor alpha mRNA. *Mol. Cell. Biol.* **19**, 4311-4323.

Laney, J. D. and Hochstrasser, M. (1999). Substrate targeting in the ubiquitin system. *Cell* **97**, 427-430.

Lin, R. (2003). A gain-of-function mutation in oma-1, a C. elegans gene required for oocyte maturation, results in delayed degradation of maternal proteins and embryonic lethality. *Dev. Biol.* **258**, 226-239.

Maduro, M. and Pilgrim, D. (1995). Identification and cloning of unc-119, a gene expressed in the Caenorhabditis elegans nervous system. *Genetics* **141**, 977-988.

Maduro, M. F., Meneghini, M. D., Bowerman, B., Broitman-Maduro, G. and Rothman, J. H. (2001). Restriction of mesendoderm to a single blastomere by the combined action of SKN-1 and a GSK-3beta homolog is mediated by MED-1 and -2 in C. elegans. *Mol. Cell* **7**, 475-485.

Maeda, I., Kohara, Y., Yamamoto, M. and Sugimoto, A. (2001). Large-scale analysis of gene function in Caenorhabditis elegans by high-throughput RNAi. *Curr. Biol.* **11**, 171-176.

Marin, V. A. and Evans, T. C. (2003). Translational repression of a C. elegans Notch mRNA by the STAR/KH domain protein GLD-1. *Development* **130**, 2623-2632.

Mello, C. C., Draper, B. W., Krause, M., Weintraub, H. and Priess, J. R. (1992). The pie-1 and mex-1 genes and maternal control of blastomere identity in early C. elegans embryos. *Cell* **70**, 163-176.

Mello, C. C., Schubert, C., Draper, B., Zhang, W., Lobel, R. and Priess, J. R. (1996). The PIE-1 protein and germline specification in C. elegans embryos. *Nature* **382**, 710-712.

Musti, A. M., Treier, M. and Bohmann, D. (1997). Reduced ubiquitin-dependent degradation of c-Jun after phosphorylation by MAP kinases. *Science* **275**, 400-402.

Nishi, Y. and Lin, R. (2005). DYRK2 and GSK-3 phosphorylate and promote the timely degradation of OMA-1, a key regulator of the oocyte-to-embryo transition in C. elegans. *Dev. Biol.* **288**, 139-149.

Ogura, K., Kishimoto, N., Mitani, S., Gengyo-Ando, K. and Kohara, Y. (2003). Translational control of maternal glp-1 mRNA by POS-1 and its interacting protein SPN-4 in Caenorhabditis elegans. *Development* **130**, 2495-2503.

Pagano, J. M., Farley, B. M., McCoig, L. M. and Ryder, S. P. (2007). Molecular basis of RNA recognition by the embryonic polarity determinant MEX-5. *J. Biol. Chem.* **282**, 8883-8894.

Page, B. D., Guedes, S., Waring, D. and Priess, J. R. (2001). The C. elegans E2F- and DP-related proteins are required for embryonic asymmetry and negatively regulate Ras/MAPK signaling. *Mol. Cell* **7**, 451-460.

Pickart, C. M. (2001). Mechanisms underlying ubiquitination. *Annu. Rev. Biochem.* **70**, 503-533.

Praitis, V., Casey, E., Collar, D. and Austin, J. (2001). Creation of low-copy integrated transgenic lines in Caenorhabditis elegans. *Genetics* **157**, 1217-1226.

Priess, J. R. and Thomson, J. N. (1987). Cellular interactions in early C. elegans embryos. *Cell* **48**, 241-250.

Puig, S., Askeland, E. and Thiele, D. J. (2005). Coordinated remodeling of cellular metabolism during iron deficiency through targeted mRNA degradation. *Cell* **120**, 99-110.

Pulak, R. and Anderson, P. (1993). mRNA surveillance by the Caenorhabditis elegans smg genes. *Genes Dev.* **7**, 1885-1897.

Reese, K. J., Dunn, M. A., Waddle, J. A. and Seydoux, G. (2000). Asymmetric segregation of PIE-1 in C. elegans is mediated by two complementary mechanisms that act through separate PIE-1 protein domains. *Mol. Cell* **6**, 445-455.

Robertson, S. M., Shetty, P. and Lin, R. (2004). Identification of lineage-specific zygotic transcripts in early Caenorhabditis elegans embryos. *Dev. Biol.* **276**, 493-507.

Rose, L. S. and Kemphues, K. J. (1998). Early patterning of the C. elegans embryo. *Annu. Rev. Genet.* **32**, 521-545.

Schubert, C. M., Lin, R., de Vries, C. J., Plasterk, R. H. and Priess, J. R. (2000). MEX-5 and MEX-6 function to establish soma/germline asymmetry in early C. elegans embryos. *Mol. Cell* **5**, 671-682.

Seydoux, G. and Fire, A. (1994). Soma-germline asymmetry in the distributions of embryonic RNAs in Caenorhabditis elegans. *Development* **120**, 2823-2834.

Shirayama, M., Soto, M. C., Ishidate, T., Kim, S., Nakamura, K., Bei, Y., van den Heuvel, S. and Mello, C. C. (2006). The conserved kinases CDK-1, GSK-3,

KIN-19, and MBK-2 promote OMA-1 destruction to regulate the oocyte-to-embryo transition in C. elegans. *Curr. Biol.* **16**, 47-55.

Sonnichsen, B., Koski, L. B., Walsh, A., Marschall, P., Neumann, B., Brehm, M., Alleaume, A. M., Artelt, J., Bettencourt, P., Cassin, E. et al. (2005). Full-genome RNAi profiling of early embryogenesis in Caenorhabditis elegans. *Nature* **434**, 462-469.

Stitzel, M. L., Pellettieri, J. and Seydoux, G. (2006). The C. elegans DYRK kinase MBK-2 marks oocyte proteins for degradation in response to meiotic maturation. *Curr. Biol.* **16**, 56-62.

Strome, S., Powers, J., Dunn, M., Reese, K., Malone, C. J., White, J., Seydoux, G. and Saxton, W. (2001). Spindle dynamics and the role of gamma-tubulin in early Caenorhabditis elegans embryos. *Mol. Biol. Cell* **12**, 1751-1764.

Tenenhaus, C., Schubert, C. and Seydoux, G. (1998). Genetic requirements for PIE-1 localization and inhibition of gene expression in the embryonic germ lineage of Caenorhabditis elegans. *Dev. Biol.* **200**, 212-224.

Tenlen, J. R., Schisa, J. A., Diede, S. J. and Page, B. D. (2006). Reduced dosage of pos-1 suppresses Mex mutants and reveals complex interactions among CCCH zinc-finger proteins during Caenorhabditis elegans embryogenesis. *Genetics* **174**, 1933-1945.

Wicks, S. R., Yeh, R. T., Gish, W. R., Waterston, R. H. and Plasterk, R. H. (2001). Rapid gene mapping in Caenorhabditis elegans using a high density polymorphism map. *Nat. Genet.* **28**, 160-164.

Zhong, Q., Gao, W., Du, F. and Wang, X. (2005). Mule/ARF-BP1, a BH3-only E3 ubiquitin ligase, catalyzes the polyubiquitination of Mcl-1 and regulates apoptosis. *Cell* **121**, 1085-1095.